Numerical Studies on Saturated Kink and Sawtooth Induced Fast Ion Transport in JET ITER-like Plasmas

P. J. Bonofiglo¹, M. Podestà¹, M. Vallar², N. N. Gorelenkov¹, V. Kiptily³, R. B. White¹, C. Giroud³, S. Brezinsek⁴, and JET Contributors^{*}

¹Princeton Plasma Physics Laboratory, Princeton, NJ 08543, USA

E-mail: pbonofig@pppl.gov

27 January 2022

Abstract. This presentation examines the energetic particle transport induced by saturated kink modes and sawtooth crashes in JET deuterium plasmas. It is known that kink mode-resonant transport and phase-space redistribution from sawtooth crashes can drive strong fast ion transport with dependencies on particle pitch and energy. Measurements with JET's Faraday cup fast ion loss detector array have shown that the internal kink growth phase preceeding sawtooth crashes produces substantial fast ion losses. This report will numerically investigate the dominant energetic particle transport mechanism with a detailed examination of the fast ion phase-space dependencies, resonances, topological effects, and induced losses associated with the long-lived, resonant, kink mode and nonresonant sawtooth crash. The ORBIT-kick model forms the basis of the transport studies with realistic fast ion distributions produced from TRANSP. A recently created reduced model for sawtooth induced transport is used while the saturated kink modes are modeled with ideal MHD codes. The simulations were further validated against experiment with a newly developed synthetic Faraday cup fast ion loss detector in addition to scintillator probe and neutron measurements.

Submitted to: Nucl. Fusion

 $^{^2\}rm Ecole$ Polytechnique Fédérale de Lausanne, Swiss Plasma Center, CH-1015 Lausanne, Switzerland

 $^{^3\}mathrm{Culham}$ Centre for Fusion Energy of UKAEA, Culham Science Centre, Abingdon, UK

 $^{^4}$ Forschungszentrum Jülich, Institut für Energie-und Klimaforschung - Plasmaphysik, 52425 Jülich, Germany

^{*}See the author list of 'Overview of JET results for optimising ITER operation' by J. Mailloux et al. to be published in Nuclear Fusion Special issue: Overview and Summary Papers from the 28th Fusion Energy Conference (Nice, France, 10-15 May 2021

1. Introduction

It is well known that magnetohydrodynamic (MHD) instabilites can induce energetic particle transport and reduce confinement. The fast ion transport can be substantial enough to reduce heating and current drive, and, in extreme cases, cause wall damage from lost particle flux. Understanding and mitigating the associated fast ion transport from these phenomena is crucial for achieving a sustained reactor plasma. Additionally, tokamak reactor designs utilize external neutral beam injection (NBI) and ion cyclotron resonant heating (ICRH) schemes which further complicates energetic particle transport studies since distinctions betweeen the lower energy NBI-born fast ions and higher energy fusion products and RF-heated ions needs to be determined.

Kink modes and sawtooth crashes are common MHD instabilites which have become ubiquitous in fusion plasmas. Plasmas with weak magnetic shear and strong plasma beta are often desired and give rise to kink modes. Sawteeth are often purposefully introduced in scenario development as a constraint on the internal magnetics/q-profile. Often, the two instabilities may coexist in which the internal kink mode acts as a precursor to sawtooth crashes. This has been observed in JET plasmas with low magnetic shear where quiescent periods between sawtooth crashes give rise to slow growing kink modes which saturate prior to each crash.[1]

Internal kink modes and sawteeth have previously been reported to alter the fast ion distribution and produce measureable losses.[2, 3] The mechanisms of transport differ between resonant [4, 5, 6] and non-resonant [7, 8] processes for the two instabilities. The kink and sawtooth crash have preferences for the mode-resonant or energetic particle phase-space redistribution/stohastization induced transport. It has been observed that each process has preferences in particle pitch and energy.[9] In particular, recent work on another JET discharge has shown that the combination of non-resonant and resonant transport appear to matter and ocur at relatively large energies.[10]

This paper utilizes recently developed reduced integrated models to diagnose saturated kink mode and sawtooth induced fast ion transport in JET ITER-like plasmas. The reduced models provide a powerful foundation on which to perform energetic particle transport studies. Previous work has already examined the models' functionality and effectiveness. The reduced transport models occur within the ORBIT-kick framework [11, 12] with initial energetic particle distribution functions provided from TRANSP simulations [13]. Furthermore, the transport models have been validated against experimental fast ion loss measurements to pro-

vide a direct, quantitative, verification of the associated mode structure and amplitude. Energetic particle loss measurements further reveal differences between NBIborn ions and fusion products.

Section 2 will describe the discharge of interest and its relevant properties. The next section will also inlude measurements from fast ion loss detectors which highlight energetic particle losses associated with the saturated kink mode and sawteeth. Section 3 will examine the fast ion transport associated with the saturated kink mode with the reduced modeling. Section 4 will do the same with sawooth induced transport. Lastly, the paper will conclude with a brief summary of the results obtained and a discussion of the merits.

2. Experimental Scenario

A deuterium high performance ITER-like discharge with Ne seeding from was selected as a reference discharge.[14] Pulse 97493 includes high external heating with 30 MW of deuterium fueled NBI and 5 MW ICRH. Exhibited in Figure 1 the pulse exhibits a prolonged stable period marked by strong MHD activity. Subplot (d) shows the global neutron rate which is characterized by a "wavy" pattern of ups and downs. These correlate with sawtooth crashes as confirmed in electron temperture changes via electron cyclotron emmission (ECE) and soft x-ray (SXR). Magnetic Mirnov spectra, shown in subplot (e), display strong low frequency MHD activity. Discontinuous breaks in the spectroscopic signal further denote the sawtooth crashes.

The low frequency modes were identified as ideal kink modes via ECE and SXR measurements discussed more in reference [3]. The dominant mode has toroidal mode number n=1 at a frequency of about 11 kHz. Evident in Figure 1, the kink modes saturate and act as precursors to the sawtooth crashes. The two instabilites provide the means for both resonant and non-resonant transport for analysis. Discussed extensively in reference [3], the saturated kink modes give rise to measureable fast ion losses in JET's Faraday cup fast ion loss detector [15] and scintillator probe [16].

The discharge presents reliable loss measurements which have been used to validate the transport model in Section 2.[3]. Figure 2 presents the CCD-scintillator image from pulse 97493 at a time between sawteeth when the kink mode is observed to be strong. The recorded losses appear in two distinct regions: at low gyroradius (~ 3 cm) and at high gyroradius (~ 12 cm) with pitch angle around 60-85°. The low gyroradius region corresponds to low energy beamborn ions while the high gyroradius region corresponds

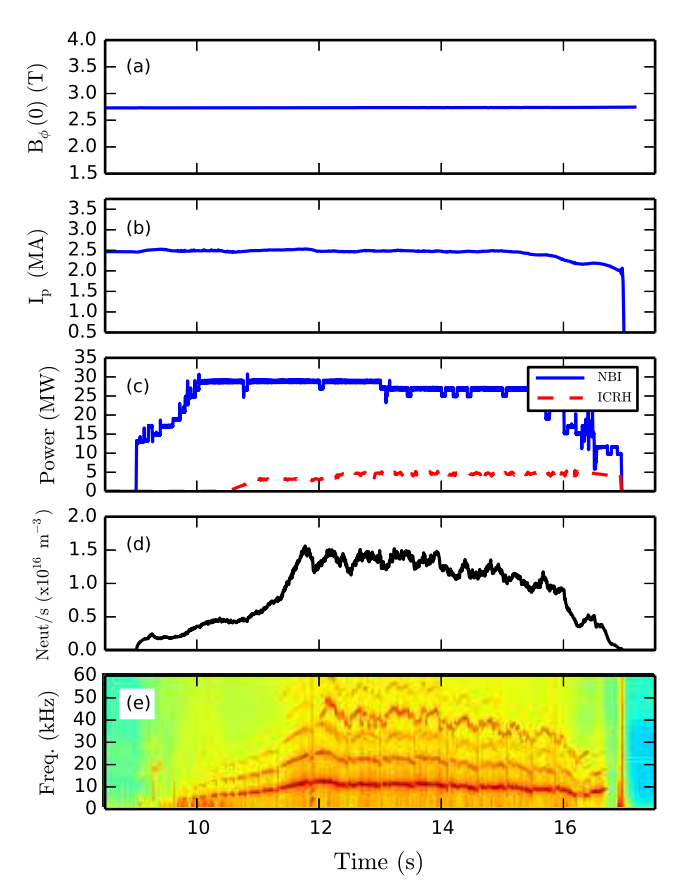


Figure 1. Basic plasma parameters for JET pulse 97493: toroidal field on axis, (a), plasma current, (b), external heating powers, (c), neutron rate, (d), and edge magentic Mirnov spectrum, (e).

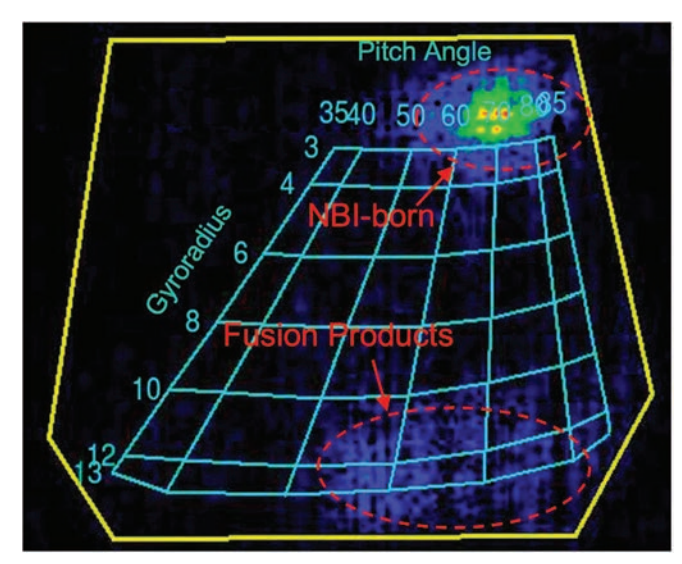


Figure 2. Scintillator fast ion loss detector signal from pulse 97493 at 13.25 sec as a function of gyroradius and pitch. Two regions are labeled for the corresponding signal from NBI-born particles and fusion products.

to high energy ions (i.e. fusion products and RF-heated deuterons). While the Farady cup fast ion

loss detector provides a wide spatial breadth, the scintillator probe measurements offer losses with a finer resolution of pitch and energy which is more sensitive to the transport studies at hand. Figure 2 shows that the losses during the time of the kink mode are stronger for the beam-born ions than the fusion products. While the kink mode induced transport could be a factor, the much larger particle content of beam-born ions may provide a simpler answer. Regardless, the presence of both signals indicate energetic particle transport.

Examining the individual photomultiplier tube (PMT) signals from the CCD-PMT array can provide further detail as a function of time. Figure 3 presents the PMTs associated with the low and high energy regions of Figure 2 as well as the total integrated CCD signal. The signals have been appropriately smoothed to remove high frequency noise. Clearly, the total CCD

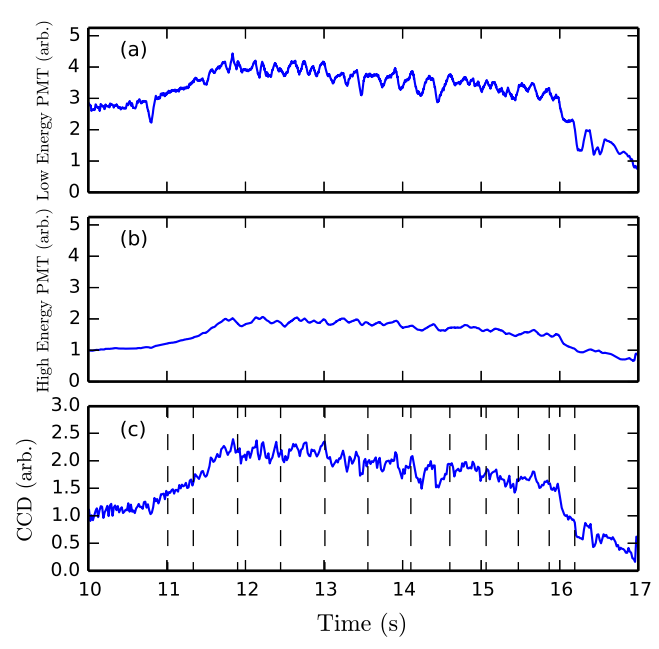


Figure 3. Scintillator fast ion loss detector signals for pulse 97493 from a low energy PMT, (a), a high energy PMT, (b), and the total integrated CCD signal, (c). The dashed vertical lines denote the times of the sawtooth crashes found from ECE and SXR signals.

signal is dominated by the low energy component which is consistent with the colored intensity of Figure 2. Additionaly, the high energy loss signal appears relatively flat while the low energy component exhibits more fluctuations. The dashed lines in subplot (c) denote the respective times of sawtooth crashes within the discharge. While not every sawtooth crash corresponds to a distinct change in the fast ion loss signal, some moulations appear consistent with the crashes. This implies the sawtooth induced transport predominantly affects the beam-born population but only mildly so that the resulting losses are minimal comparative to the prolonged kink induced losses.

Overall, the discharge presents measureable losses consistent with the kink mode and sawtooth crashes which indicate outward, radial, transport of the fast ions. The loss measurements ultimately provide experimental data on which the reduced modeling studies are based. Sections 3 and 4 will now discuss the reduced transport modeling simulations in greater detail so as to explain the observed fast ion losses and identify the associated transport.

3. Saturated Kink Mode Induced Transport

The time slice for the saturated kink mode analysis for taken at 13.8 s which occurs between two sawtooth crashes and exhibits strong measured fast ion losses. The magnetic safety factor, electron density, and temperature profiles were taken from a TRANSP simulation and were constrained against experimental measurements. While internal magnetic measurements were lacking, the q-profile was constrained due to the known sawtooth crashes and measurements of the q=1 inversion radius with ECE and SXR diagnostics. The resulting profiles are shown in Figure 4. Of note, the

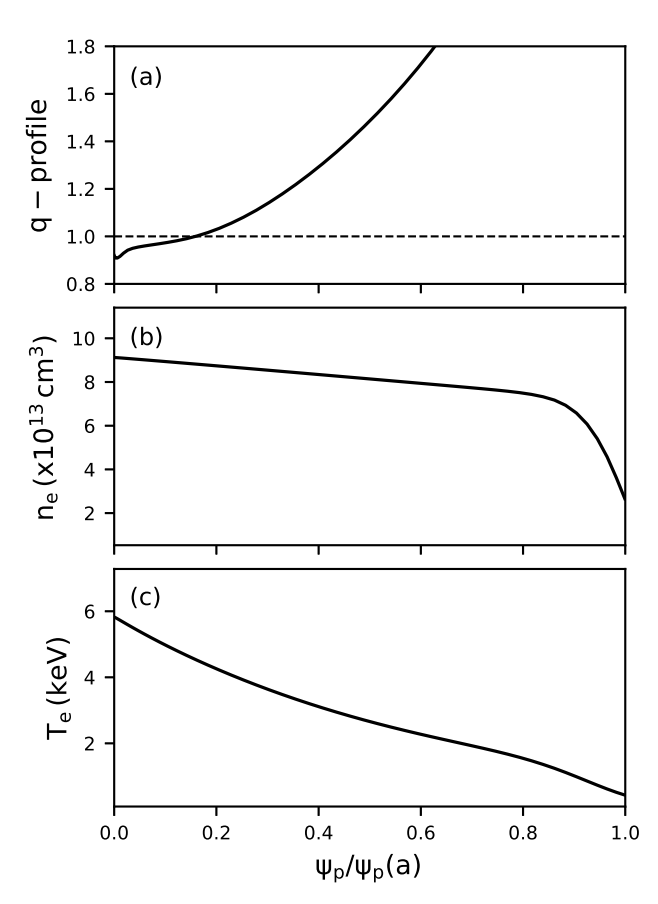


Figure 4. Q-profile, (a), electron density, (b), and electron temperature (c) computed from TRANSP for shot 97493 at 13.8 sec.

q=1 surface is relatively core-localized which will have

an impact on the sawtooth induced transport discussed in the next section. Furthermore, the density profile is flat with a high edge pedestal. This has a substantial impact on the beam-born population and the resulting transport.

The high edge density results in weak neutral beam penetration and strong edge deposition. The energetic deuteron distribution as computed from TRANSP is shown in Figure 5. The beam deposition,

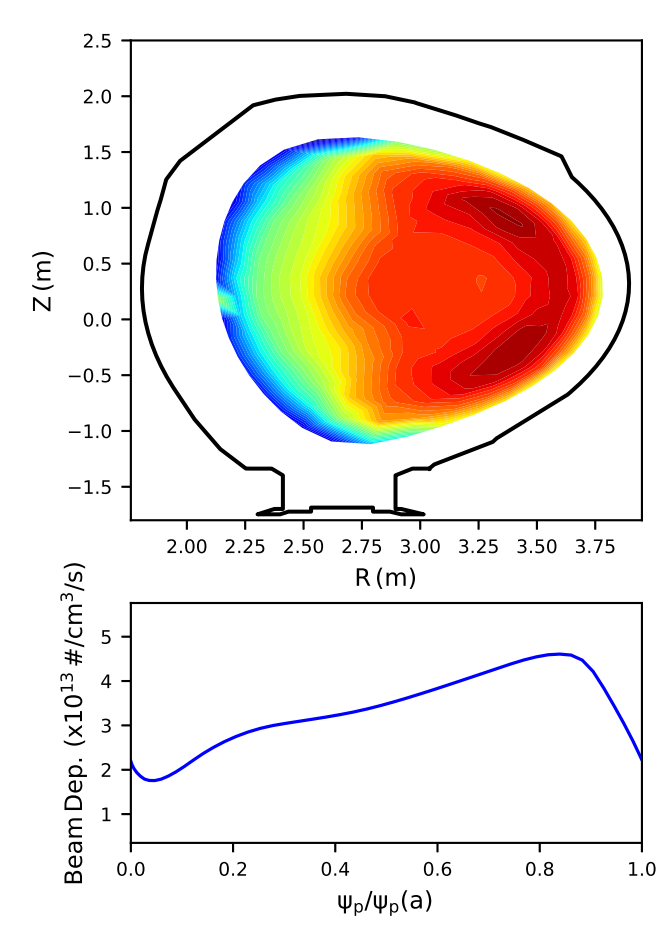


Figure 5. Fast deuteron distribution, (a), and beam deposition profile, (b), as computed by TRANSP for shot 97493 at 13.8 sec.

subplot (b), is peaked near the edge as a result of the high edge density. This results in the fast deuteron distribution in suplot (a). The distribution is relatively broad as a function of minor radius and peaks off-axis. As will be discussed, this will have a strong impact on the resulting fast deuteron resonances and transport.

The mode structure for the ideal kink mode was found with the NOVA code[17], and comparisons to ECE and fast ion loss mesurements constrained the mode amplitude. For simplicity, only the n=1 mode is considered for analysis. The mode structure (normalized radial displacement) computed with NOVA is shown in Figure 6 and contains the first three poloidal harmonics, m=1-3. The mode structure

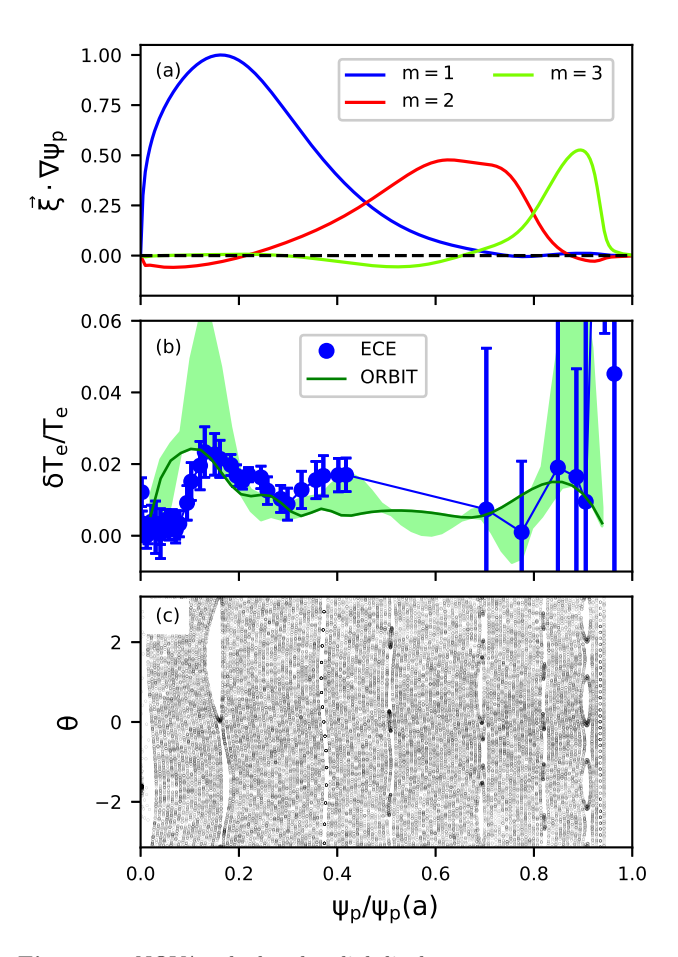


Figure 6. NOVA calculated radial displacement

exhibits a dominant, core-localized, m=1 component with subdominant m = 2,3 components extending radially outward. Subplot (b) presents the temperature fluctuations from ECE measurements (blue) and ORBIT analysis (green). The ORBIT temperature fluctuations were found initializing electron orbits with reference to the electron temperature profile from TRANSP. The resulting motion due to the applied perturbation is then tracked and correlated to a corresponding temperature fluctuation. This methodology follows that used in references in [18] and [19]. The agreement between measurment and ORBIT simulations occurred for a mode amplitude of $b/B \sim 10^{-3}$. This was further confirmed against fast ion loss measurements in reference [3]. The resulting 2D structure in (θ, ψ_n) can be observed in the magnetic Poincaré plot in subplot (c).

With the kink mode structure and amplitude determined, the energetic particle resonances can be analyzed. Using the mode structure and ampitude presented in Figure 6, Figure 7 shows kinetic energetic particle Poincaré plots for NBI-born ions as well as D-D fusion products. As expected, the fast ion resonances exhibit strong differences from the magnetics in Figure

6 (c). Since the mode can alter the fast ion's energy, multiple energy components are displated in the Poincaré plots via different colors in order to highlight the topology differences associated with the energy changes. The energies vary around ± 20 -40 keV which stems from the maximum change in energy as calculated from the ORBIT-kick model [11, 12].

The lower energy beam-born ions, subplot (a), do not resonate with the core-localized m=1 component while the m=2 and m=3 resonances are present. This is consistent with the broad beamborn distribution which peaks closer to the last closed flux surface (also pictured in 9). Meanwhile, the higher energy deuterons, tritons, and protons exhibit a strong resonance with the m=1 component. This is due to the their more core-localize distribution (see Figure 9). All particles demonstrate good confinement near the core, however, as closed surfaces are observed. Only near mid-radius to the edge due the orbits begin to stochasticize implying strong radial transport.

The above is directly observed in the examination of the strength of the resonant interaction via the ORBIT-kick code. Figure 8 presents the strength of the interaction between the kink mode and fast ions within the fast ions' constants of motion space (energy - E, magnetic moment - μ , canonical toroidal momentum - P_{ϕ}). In this manner, the interaction can be directly correlated to the various orbit topologies denoted by the magenta lines. The color scales are identical for each subplot. The initial particle sampling has been convolved against the original TRANSP calculated fast ion distribution, so not all of fast ion phase-space is covered. The beam-born ions are much more prevalent and cover most of phase-space but result in weaker interactions. The stronger interactions are near the last closed flux surface in the trapped particle domain. This is consistent with the m=2-3 resonances observed in Figure 7 and fast ion loss modeling presented in [3]. The higher energy ions maintain steeper density gradients near the core for strong m=1 interactions near the magnetic axis and largely affect co-passing orbits.

While Figure 8 presents strong core interactions for the high energy particles, the Poincaré plots from Figure 7 demonstrate that these resonances are relatively well confining. Particles pushed outward toward larger radii and trapped/stagnation/counterpassing exhibit reduced/weaker resonances but more orbit stochasticity as the modes overlap. Moreso, the overlap grows when extensions to other energies are included presented in the different colors of Figure 7.

The global transport is also evident in the change in the 1D fast ion density profiles. Figure 9 portrays the change in the energetic particle profiles as calculated in ORBIT due to the saturated kink mode. The initial profiles were taken from the TRANSP

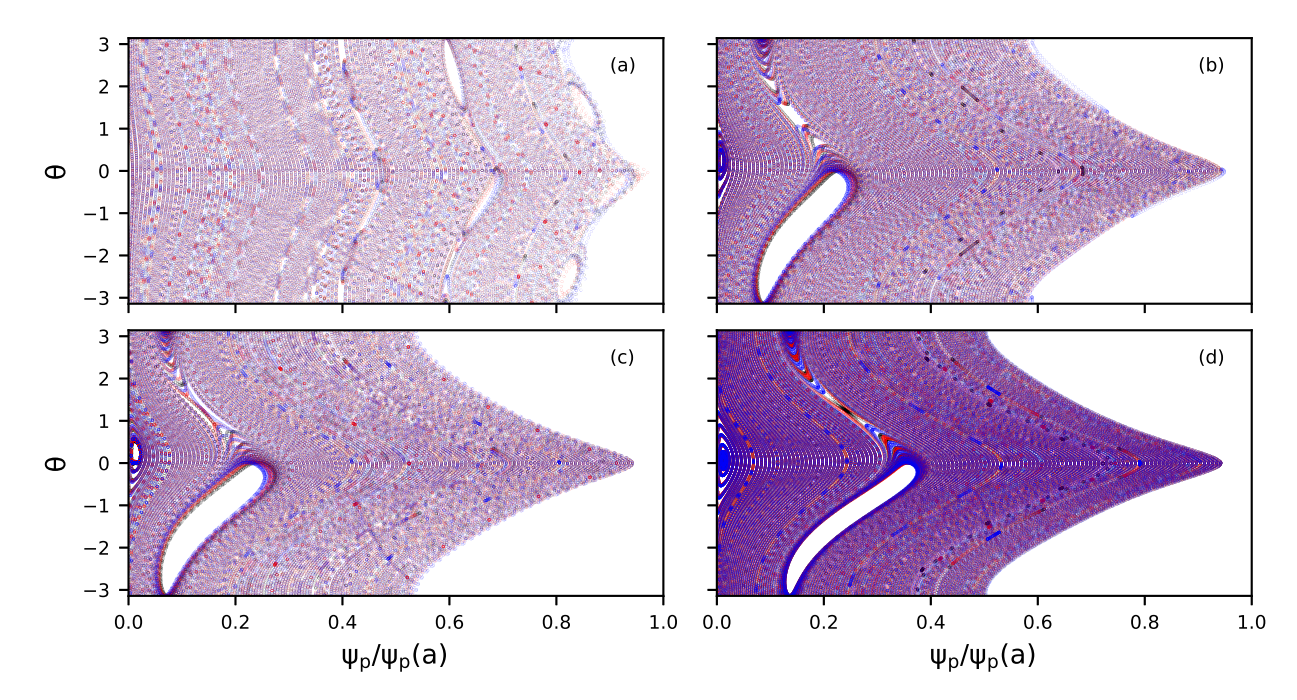


Figure 7. Kinetic energetic particle Poincaré plots for 120 keV deuterons, (a), 1000 keV deuterons, (b), 1000 keV tritons, (c), and 3000 keV protons, (d), found with the mode structure in Figure 6 at $\mu B_0/E = 0.8$. Blue points represent a downard shift in energy of 20-40 keV and red points represent an upward shift in energy of 20-40 keV based on the largest resonant changes computed from ORBIT-kick.

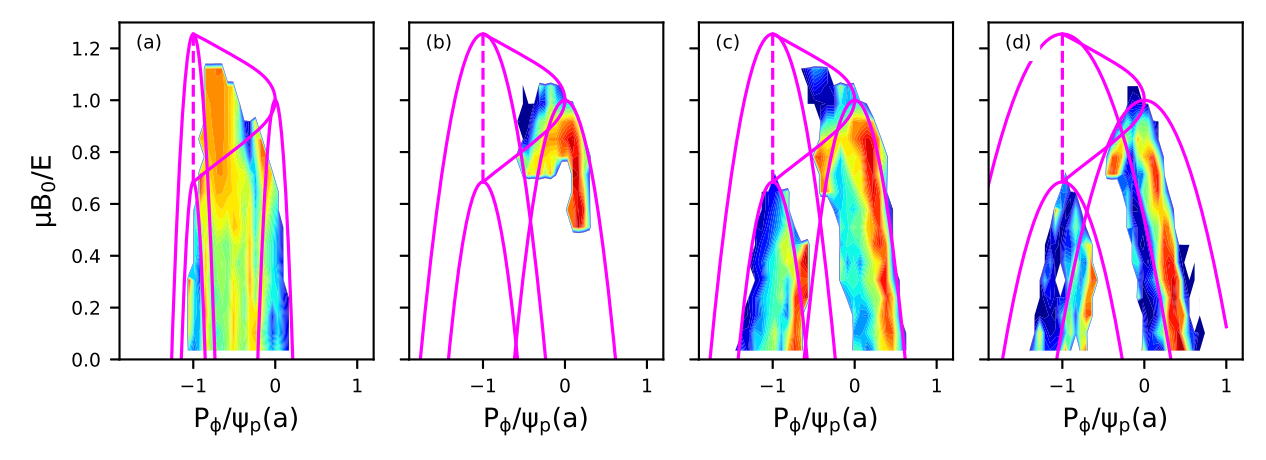


Figure 8. Strength of the resonant kink interaction for 120 keV deuterons, (a), 1000 keV deuterons, (b), 1000 keV tritons, (c), and 3000 keV protons, (d), as calculated from the ORBIT-kick model. The orbit topology boundaries are plotted in magenta.

distributions. Hinted at in Figure 5, the deuteron distribution is relatively flat and is acctually somewhat hollow as it peaks near $\psi_p/\psi_p(a)\approx 0.7$. The flat spatial gradient should lacks a free energy source to destabilize energetic particle modes and should produce weaker fast ion resonances.[20] Subplot (a) actually shows the redistribution of deuterons as the core population reduces and off-center peakedness becomes more pronounced. The rise in edge particles should then exhibit strong resonances with the m=2-3 modes and induce losses. The fusion products are much more peaked on core where the steep gradient can exhibit a strong resonance with the m=1 component.

This leads to a clear reduction in the core-population of particles. There is a slight rise in particles near the edge which signifies the outward transport and observed losses.

This high edge pedestal present in JET discharge 97493 presents interesting transport properties between the lower energy beam-born ions and the higher energy fusion products. Namely, the fast ion distributions are markedly different. The beam deposition is located off-axis (additionally the RF-resonance is located off-axis) which flattens the deuteron fast ion profile while the fusion product profiles are peaked on-axis. This gives rise to markedly different reso-

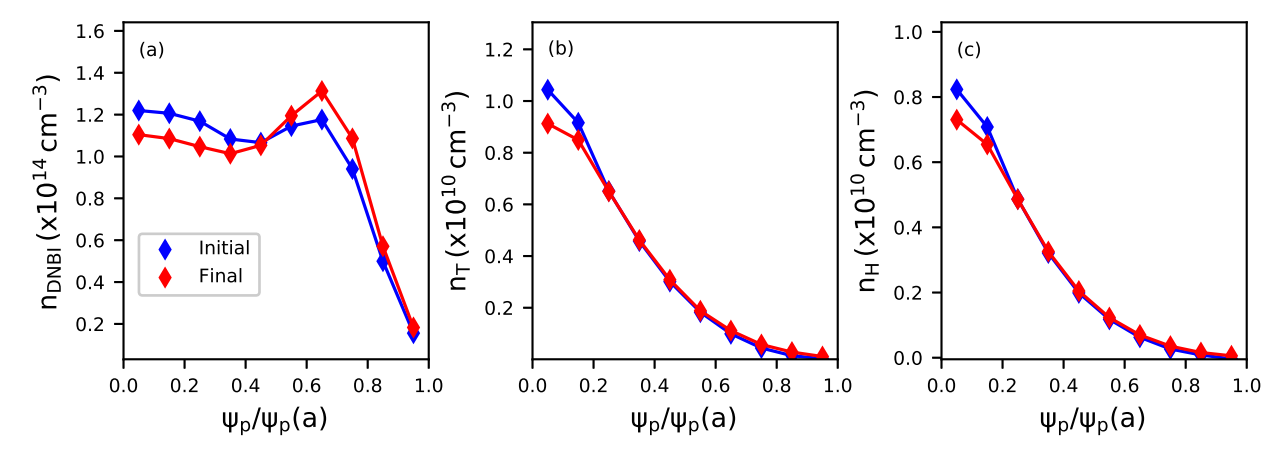


Figure 9. Change in the fast ion density profile for deuterons, (a), tritons, (b), and protons, (c) due to the saturated kink mode. Note the differences in scale between the deuterons and fusion products.

nances whereby the fusion products are the only ones to exhibit strong core-transport while beam-born ions are predominantly resonant near the edge. Poincaré plots show that all of the fast ions start to experience stochastic orbits as the resonances alter the fast ions' constants of motion (namely energy). Consequently, the saturated kink mode interacts strongest with the fusion products as opposed to the beam-born ions. The next section will now discuss the associated transport due to the sawtooth crashes.

4. Sawtooth Induced Transport

The kink modes persists throught a series of sawtooth crashes which could in turn incite further fast ion transport. Figure 10 presents the magnetic safety factor, electron density, and temperature profiles beore (blue) and after (red) a sawtooth crash in shot 97493. The same high edge pedestal is present with a drop in T_e appearent due to the eelctron transport commonly associated with the crash. The q=1 surface is relatively core-localized which will dictate the fast ion transport as layed out in the reucced sawtooth model in [18].

The sawtooth structure is taken from an analytic theory presented in [18] equation 2. This equation presents the $\alpha_{m,n}$ coefficients where $\delta \mathbf{B}_{m,n} = \nabla \times \alpha_{m,n} \mathbf{B}$. The free parameters M and P in equation 2 were taken as 0.5 and 3.0, respectively. The mode maintains a dominant n=1, m=1 structure with subdominant poloidal harmonics. The resulting radial displacement is shown in Figure 11 for the first three poloidal harmonics. The mode structure is fairly similiar to the NOVA calculated kink mode structure which is unsurprising since the formulation in [18] was constructe to match NOVA output in an NSTX-U discharge. The mode amplitude is found self-consistently within the same reduced model. The mode

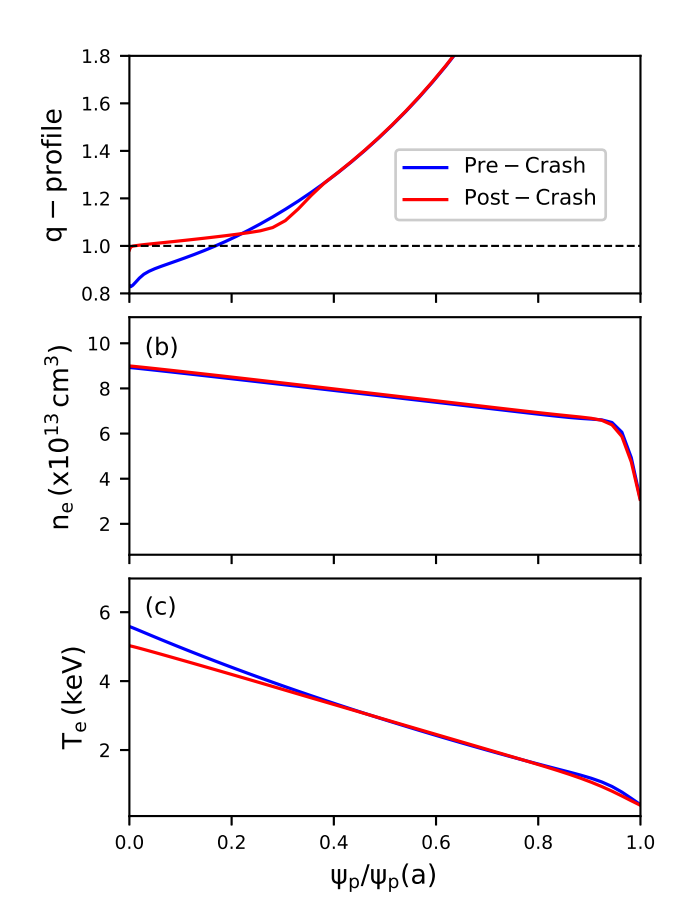


Figure 10. Q-profile, (a), electron density, (b), and electron temperature (c) computed from TRANSP for shot 97493 before and after the sawtooth crash at 13.48 sec.

amplitude is varied in time as an exponential growth followed by a rapid decay to represent the crash. The peak mode amplitude is found via mixing electron orbits from the core to the q=1 radius, i.e. full Kadomtsev reconnection. For the discharge of interest, the peak mode amplitude was found to be $\delta b/B \sim 0.17$ which is quite robust.

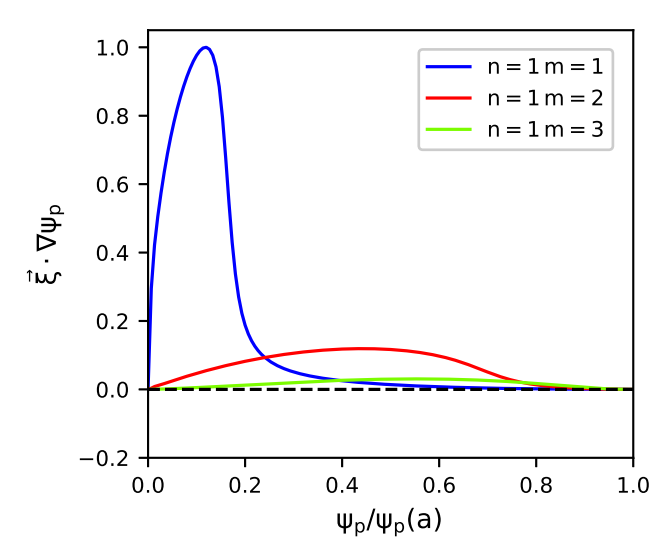


Figure 11. Radial displacement calculated from the analytic sawtooth model presented in [18] with M=0.5 and P=3.0 in equation 2.

The reduced sawtooth model of [18] was ran with the previously stated mode. The resulting energetic particle profile change across the sawtooth crash is shown in Figure 12. Again, the particles were initially seeded from the TRANSP produced distributions. The resulting redistribution is consistent with that observed in [10] and [18]. Namely, the fast ions undergo mixing around the q = 1 surface and leads to an outward transport of particles. Interestingly, the resulting change in the fast ion profiles presented in Figure 12 are much smaller than that presented in [10]. Additionally, the profiles post-crash retain their approximate slope instead of drastically flattening out which would be expected of a standard Kadomtsev model. The profiles do not change much at all near the edge; moreso for the fusion products. A barely visible rise is evident in the deuteron profile for $\psi_p/\psi_p(a) >$ 0.7 but not for the tritons or protons. This indicates a possible weak association with sawtooth induced losses for the beam-born species but not the fusion products. This is consistent with the results presented in Figure 3. Sawtooth induced losses were not strongly obersved in the Faraday cup fast ion loss array up to the noise floor as well.

The sawtooth crash redistributes fast ions as a function of pitch and energy as well. Theory [9] has shown that there exists a critical energy below which fast ions will experience non-resonant transport and be strongly redistributed. For trapped and passing particles in JET, this critical energy is of order a few hundred keV. Since $E_{NBI}=120~{\rm keV}$, beam-injected deuterons should experience sawtooth induced redistribution while higher energy RF-deuterons and fusion products should be largely

unaffected. Figure Evident in Figure 13, the deuteron distribution changes across the sawtooth crash at energies below 200 keV consistent with theory. The triton and proton distributions, however, exhibit a change in the distribution at much larger energies. Of note, there appears to be a positive change in the distribution at high pitch at energies 400-1000 keV for tritons and 1500-3000 keV for protons. Interestingly, reference [10] also observed distributional changes at high energies for a JET RF-heated discharge. Thus, it appears, that the non-resonant transport in [9] fails to portray a complete picture of the energetic particle transport picture. The resonant interactions calculated in the reduced ORBIT model produce nonnegligible perturbations in the fast ion distributions at high energy which are evident in both Figures 12 and 13. It is theorized that the deuterons do not observe redistribution above the critical energy owing to the largely flat radial profile shown in Figure 12.

The direct change in orbit topologies can again be taken directly from ORBIT. Figure 14 displays the relative change in orbit types for the various fast ion species. Possible orbit types include co-passing, counter-passing, trapped, potato/stagnation, and lost. The x-axis denotes the initial orbit while the colored bar denotes the respective fraction of the final orbit type. For example, the majority of initial counterpassing orbits for deuterons remain counter-passing while $\sim 15\%$ transfer to losses and $\sim 5\%$ change to copassinig orbits. Most orbits predominantly maintain their original topology, co-passing particles being the strongest. There exists redistribution among the confined orbits for all species. Most notably, copassing, trapped, and potato orbits tend to mix together while most losses stem from counter-passing particles. Potato/stagnation orbits undergo the most changes since the topological boundaries are relatively close together to other orbit types. These results are consistent with those observed in NSTX-U sawtooth modeling.[7]

In short, the reduced sawtooth modeling has revealed strong non-resonant transport effects which are typically not included in modeling efforts such as the standard Kadomtsev model within TRANSP. Beam-born ions undergo a modest redistribution while higher energy fusion products unergo a mild redistribution. Most of the associated transport, however, surrounds the core-localized q=1 surface so losses are minimal. These observations are consistent with experiment and previous modeling efforts.

5. Discussion and Conclusion

Energetic particle transport was analyzed for a JET ITER-like discharge due to a saturated kink mode

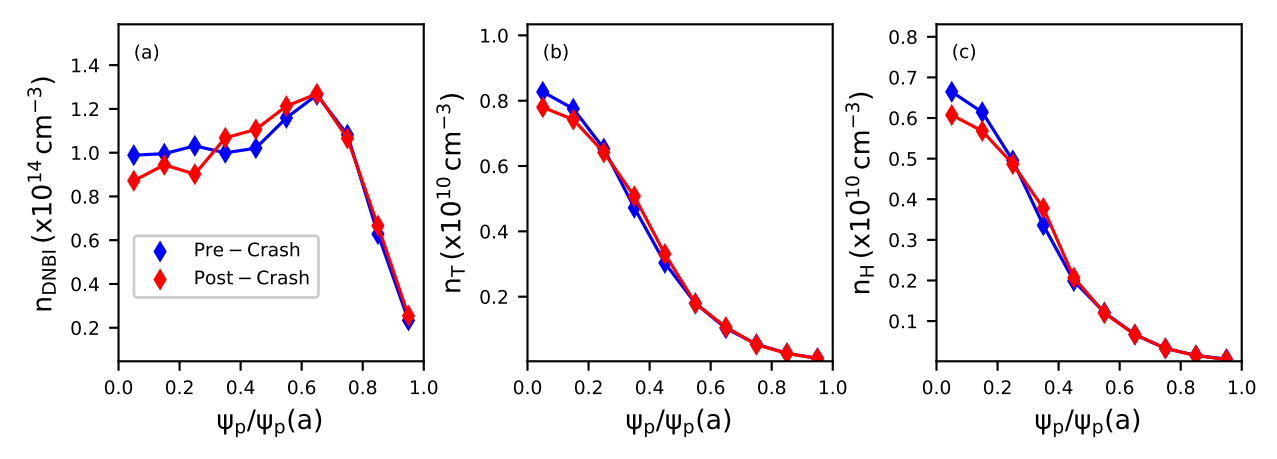


Figure 12. Change in the fast ion density profile for deuterons, (a), tritons, (b), and protons, (c) due to the ORBIT simulated sawtooth crash. Note the differences in scale between the deuterons and fusion products.

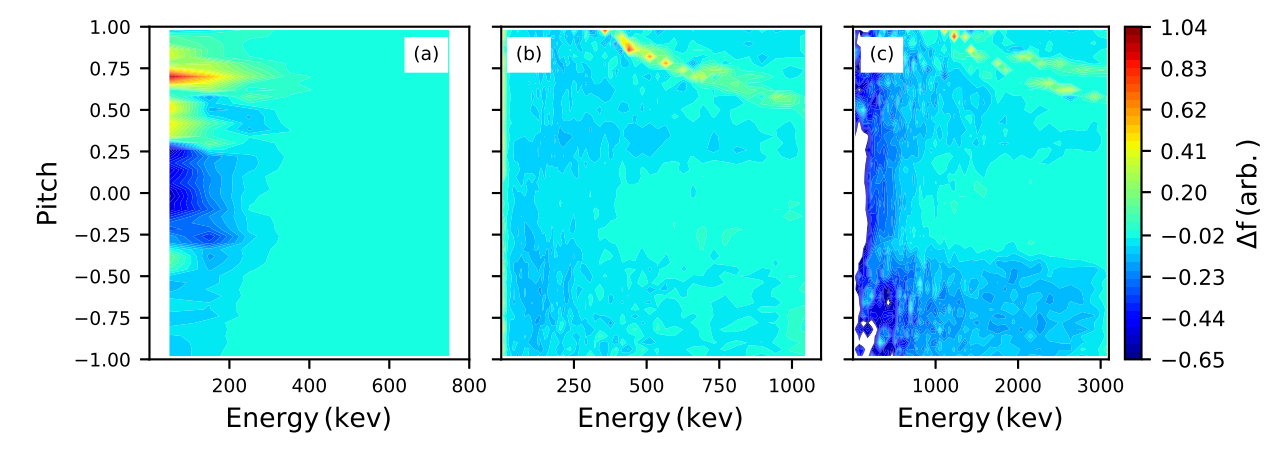


Figure 13. Change in the fast ion distribution, $\Delta f = f_{post} - f_{pre}$, for deuterons, (a), tritons, (b), and protons, (c) due to the ORBIT simulated sawtooth crash in energy and pitch at radius $\psi_p/\psi_p(a) = 0.1$.

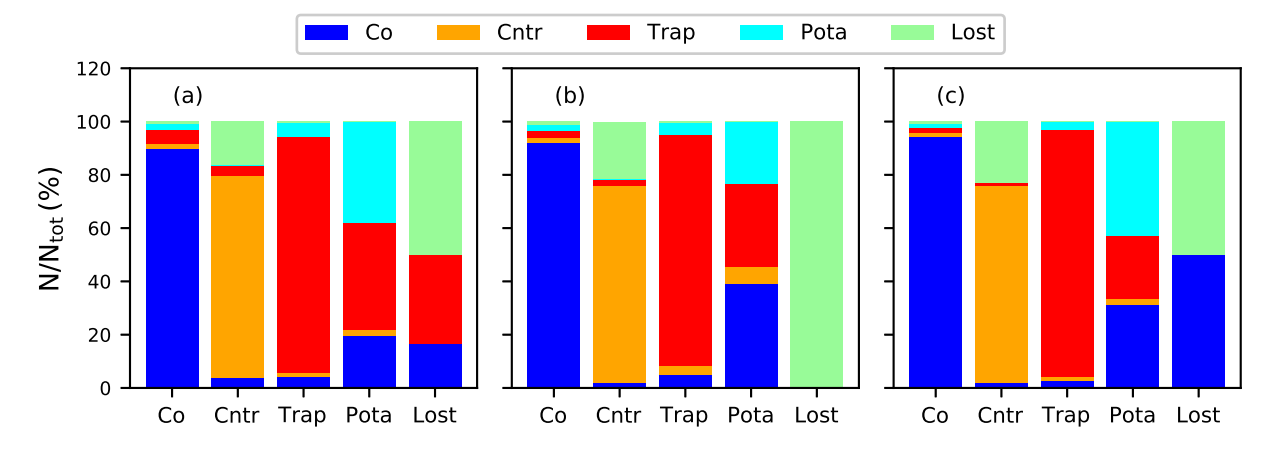


Figure 14. Change in orbit types induced by the sawtooth crash for deuterons, (a), tritons, (b), and protons, (c). The x-axis denotes the initial orbit while the colored bar denotes the respective fraction of the final orbit type. Orbit types include co-passing, counter-passing, trapped, potato/stagnation, and lost.

and sawtooth crash using newly developed reduced models. Fast ion loss measurements were used to validate and confirm model parameters and results. Kink mode induced transport was examined with a synthetic loss model and the ORBIT-kick model. High energy particles, such as fusion products, exhibited the strongest resonant interac=tions with the kink mode while beam-born particles lacked core-transport due to a broad/flat spatia profille. Orbit stochasticity became apparent near the edge as the m=2 and 3 modes overlapped with changing particle energy. Sawtooth induced transport was rather minimal as fast ions mixed across the q=1 surface but did not radially move beyond mid-radius. A pitch and energy sensitivity was observed that further indicates the sawtooth resonant transport has a strong effect. Additional modeling is desired to further reveal this dependency.

Further testing can be done to distinguish the reesonant vs. non-resonant fast ion transport. ORBIT-kick can be used to calculate the transport matrices (i.e. orbit "kicks") for each ion species and reintroduced into TRANSP. This can be done for both the resonant and non-resonant cases. The resulting relative changes in the neutron rate and energetic particle distributions could then be analyzed. In doing so, the relative importance of the resonant vs. non-resonant effects can be directly compared. Additionally, the sawtooth analysis can be performed on JET's synthetic loss model[3] to confirm or refute the lack of measured losses

The results obtained with the reduced models (ORBIT-kick, sawtooth model, synthetic loss model) highlights their robustness and usefulness. The reduced modeling framework allows for faster computation and analysis at high fidelity. Parameter tuning is quick and simple while the results shown provide meaningful physical insights. Shown within this manuscript, important distinctions must be made among the beamborn fast ions and fusion products in regards to their associated transport. This is particularly important for JET's 2021 DT-campaign which recently finished. The alpha profile is expected to be sharpyl peaked on axis which may drastically differ from the beam population. The resulting transport, mode stability, and slowing will be different among the populations as highlighted in this manuscript.

Acknowledgements

This manuscript is based upon work supported by the U.S. Department of Energy, Office of Science, Office of Fusion Energy Sciences, and has been authored by Princeton University under Contract Number DE-AC02-09CH11466 with the U.S. Department of Energy. This work has been carried out within the framework of the EUROfusion Consortium and has received funding from the Euratom research and training programme 2014-2018 and 2019-2020 under grant agreement No 633053. The views and opinions expressed herein do not necessarily reflect those of the European Commission. This work was supported in part by the Swiss National Science Foundation.

Additionally, the authors would like to thank the work of all JET task force leaders, machine operators, and diagnosticians for the shot involved in this work.

References

- [1] Buratti P et al. 2006 Plasma Phys. Control Fusion 48 1005
- 2] Jackson A R et al. 2020 Nucl. Fusion 60 126035
- [3] Bonofiglo P J et al. 2022 Nucl. Fusion **62** 026026
- [4] Kolesnichenko Y I et al. 1998 Phys. Plasmas 5 2963
- [5] Kolesnichenko Y I et al. 2000 Nucl. Fusion 40 1325
- [6] Farengo R et al. 2013 Nucl. Fusion **53** 043012
- [7] Kim D et al. 2018 Nucl. Fusion 58 082029
- [8] Kim D et al. 2019 Nucl. Fusion **59** 086007
- [9] Kolesnichenko Y I et al. 1997 Phys. Plasmas 4 2544
- [10] Teplukhina A A et al. 2021 Nucl. Fusion 61 116056
- [11] Podesta M et al. 2014 Plasma Phys. Control Fusion 56 055003
- [12] Podesta M et al. 2017 Plasma Phys. Control Fusion 59 095008
- [13] doi:10.11578/dc.20180627.4
- [14] Giroud C, Brezinsek S et al. High performance ITER-baseline discharges in deuterium with nitrogen and neon-seeding in the JET-ILW. Preprint: 2020 IAEA Fusion Energy Conference, Nice, France (12 May 2021) [EX/P3-9]
- [15] Bonofiglo P J et al. 2020 Rev. Sci. Instrum. 91 093502
- [16] Baeumel S et al. 2004 Rev. Sci. Instrum. **75** 3563
- [17] Cheng C Z and Chance M S 1986 Phys. Fluids 29 3695
- [18] Podesta M et al. 2022 Plasma Phys. Control Fusion 64 025002
- [19] Perez von Thun C et al. 2010 Nucl. Fusion 50 084009
- [20] Heidbrink W W and White R B 2020 Phys. Plasmas 27 030901